ImmunoTargets and Therapy

Dovepress
Taylor & Francis Group

Open Access Full Text Article

SHORT REPORT

Circulating miR-148a-3p Correlates with Inadequate Induction Response in Pediatric Hodgkin Lymphoma

Marius Rohde[1,*], Vijay Kumar Singh[1,*], Andrea Wolfermann[1], Birgit Burkhardt[2], Claudia Blattmann[3], Daniel Steinbach[4], Dominik T Schneider[5], Martin Ebinger[6], Britta Maecker-Kolhoff[7], Matthias Braun[1], Lars Kurch[8,9], Christine Mauz-Körholz[1,10], Dieter Körholz[1]

[1]Department of Pediatric Oncology, Hematology and Immunodeficiencies, Justus-Liebig-University, Giessen, Germany; [2]Department of Pediatric Hematology and Oncology, University Children's Hospital Muenster, Muenster, Germany; [3]Pediatric Oncology, Hematology, Immunology, Klinikum Stuttgart-Olgahospital Stuttgart Cancer Center, Stuttgart, Germany; [4]Pediatrics and Adolescent Medicine, University Medical Center Ulm, Ulm, Germany; [5]Clinic of Pediatrics, Dortmund Municipal Hospital, University Witten/Herdecke, Dortmund, Germany; [6]Department of Paediatric Hematology, Oncology, Gastroenterology, Nephrology and Rheumatology, University Children's Hospital Tübingen, Tübingen, Germany; [7]Department of Pediatric Hematology and Oncology, Hannover Medical School, Hannover, Germany; [8]Department of Nuclear Medicine, University Hospital Leipzig, Leipzig, Germany; [9]Department of Anesthesiology and Operative Intensive Care, University Hospital Halle (Saale), Halle (Saale), Germany; [10]Medical Faculty, Martin-Luther University of Halle-Wittenberg, Halle, Germany

*These authors contributed equally to this work

Correspondence: Marius Rohde, Department of Pediatric Oncology, Hematology and Immunodeficiencies, Justus-Liebig-University, Feulgenstraße 10-12, Giessen, 35392, Germany, Tel +49 641 985 43421, Fax +49 641 985 43429, Email Marius.Rohde@paediat.med.uni-giessen.de

Abstract: Pediatric Hodgkin lymphoma (HL) is highly curable, and reducing the treatment intensity in patients who respond well to induction therapy is a key strategy for minimizing long-term adverse effects. Biomarkers that identify good responders at diagnosis would enable further de-escalation of the treatment. Circulating microRNAs (miRNAs) have shown promise as noninvasive indicators of therapeutic response in hematological cancers, yet their association with early metabolic response on quantitative 18F-Fluorodeoxyglucose-Positron Emission Tomography (18F-FDG-PET) in pediatric HL has not been defined. Here, we investigated the potential of circulating miRNAs to predict the response to induction therapy in pediatric HL. Small RNA sequencing of serum samples from 35 patients revealed 24 Hodgkin lymphoma–associated miRNAs that were differentially expressed between adequate and inadequate responders. Subsequent quantitative reverse transcription-polymerase chain reaction (qRT-PCR) validation demonstrated significantly elevated miR-148a-3p levels at diagnosis in inadequate responders to induction therapy than in adequate responders (p=0.009). These results indicate that circulating miR-148a-3p may enhance current predictive approaches by identifying high-risk patients less likely to achieve rapid metabolic remission.

Keywords: pediatric cancer, classical Hodgkin lymphoma, microRNA, circulating microRNA, serum, biomarker, early response assessment quantitative positron emission tomography

Introduction

Pediatric classical Hodgkin's lymphoma (cHL) is highly curable, with an estimated five-year survival rate exceeding 90%.[1,2] Despite these favorable outcomes, approximately one-third of patients in the EuroNet-PHL trials failed to achieve an adequate metabolic response, measured by quantitative 18F-Fluorodeoxyglucose-Positron Emission Tomography (18F-FDG-PET), after two cycles of induction chemotherapy with vincristine, etoposide, prednisone, and doxorubicin (OEPA), necessitating intensified consolidation chemotherapy and radiotherapy to ensure durable remission.[1,2] However, the biological mechanisms driving these distinct responses to induction therapy are not well defined.

https://doi.org/10.2147/ITT.S577426
Received: 1 November 2025
Accepted: 3 March 2026
Published: 1 April 2026

Circulating microRNAs (miRNAs) — around 22-nucleotide noncoding RNAs — have emerged as promising, minimally invasive biomarkers for cancer diagnosis, prognosis, and therapy monitoring[3] due to their high stability in blood and regulatory role in gene expression.[4] In classical Hodgkin's lymphoma (HL), studies have identified aberrant miRNA expression in both tissue and cell-free samples that contributes to pathogenesis by influencing immune evasion, loss of B-cell phenotype, drug sensitivity and resistance, and activation of growth-promoting pathways via the regulation of target genes.[5,6] Based on this evidence, we hypothesized that specific circulating miRNA signatures may reflect tumor biology and can predict early therapeutic outcomes in pediatric patients.

Therefore, this study investigates whether serum miRNA expression at diagnosis correlates with the early metabolic response to induction chemotherapy in pediatric cHL.

Materials and Methods

To test this hypothesis, serum miRNA profiles were analyzed in a cohort of 35 newly diagnosed pediatric HL patients in the EuroNet-PHL-C2 trial (EudraCT: 2012–004053-88). Biobank serum samples were collected across multiple German centers with written informed consent from participants or legal guardians, processed within 24 h, and stored at −80 °C. Only samples without visible hemolysis were included. The cohort (ages 3.4–18 years; male:female ≈1.5:1) predominantly presented with stage II disease (60%), with stages III and IV each comprising 20%. Elevated ESR was observed in 57%, B-symptoms in 40%, bulky disease in 43%, and extranodal involvement in 31% (Table S1). These baseline characteristics were comparable to those observed in clinical studies.

All patients underwent OEPA chemotherapy followed by 18F-FDG-PET–based early response assessment (ERA).[1] Metabolic response was quantified using the lesion-to-liver activity ratio (qPET), applying a threshold of 1.3 to distinguish adequate from inadequate metabolic response.[7] Patients with qPET <1.3 were classified as ERAqPET-negative or adequate responders (AR) (n=13), and those with qPET ≥1.3 as ERAqPET-positive or inadequate responders (IR) (n=22) (Table S1).

Peripheral blood was collected at diagnosis (day 0) and post-induction (day 57). Serum was isolated by double centrifugation to remove debris and platelets and stored at −80 °C. Total RNA, including miRNAs, was extracted using the miRNeasy Serum/Plasma Kit (Qiagen). Minimal hemolysis was confirmed (ΔCt miR-23a–miR-451a <5),[8] and stable endogenous miRNA recovery was verified across samples (Figure S1A–C).

Small RNA libraries were prepared using the QIAseq-miRNA Library Kit (Qiagen), quantified by qRT-PCR, and sequenced (single-end 75 bp reads) on an Illumina NextSeq-500 (Illumina, Inc). Reads were trimmed, aligned to GRCh37, and annotated using miRBase 20.[9] On average, 488 miRNAs per sample were detected at ≥1 TPM (Figure S2A), consistent with previous serum miRNA studies.[10] Data were normalized using the trimmed mean of M-values (TMM), and differential expression analysis was performed using edgeR (Bioconductor).[11] Principal component analysis (PCA) identified three technical outliers (using PCA score-plot: Hotelling T^2 test), which were excluded from downstream analyses (Figure S2B).

Expression of miR-148a-3p was validated using qRT-PCR (Qiagen). RNA was reverse-transcribed and amplified according to manufacturer instructions, and expression was calculated using the $2^{-}\Delta\Delta$Ct method (Ct < 38; GeneGlobe, Qiagen). Values were normalized to the global Ct mean and compared with ERAqPET-negative controls. Diagnostic performance was assessed using receiver operating characteristic (ROC) curve analysis, with area under ROC curve (AUROC) used to determine sensitivity and specificity. Statistical analyses were performed using Mann–Whitney *U*-tests, linear regression and Spearmann correlation, with data visualization conducted in R and GraphPad Prism 10 (San Diego, CA, USA). Statistical significance was defined as $p < 0.05$.

Results

Pre-induction serum sequencing identified 173 miRNAs with a TMM ≥50, of which 119 were reported in adult HL studies (Table S2). A comparison of these 119 miRNAs in the ERAqPET subgroups revealed 24 HL-associated miRNAs with divergent baseline expressions (Table 1). Among these, ten miRNAs—including miR-223-3p, miR-143-3p, miR-345-5p, miR-24-3p, miR-629-5p, miR-140-5p, miR-148a-3p, miR-190b, miR-181a-5p, and miR-27b-3p—were elevated at diagnosis in inadequate responders, whereas fourteen—miR-4732-3p, miR-144-3p, let-7e-5p, miR-103a-3p, let-7f-5p,

Table 1 Expression of Differentially Expressed miRNAs Between ERAqPET Negative and ERAqPET Positive Patients' Samples Before Start of Induction Therapy

miRNAs	ERAqPET Negative (in TMM)	ERAqPET Positive (in TMM)	Fold Expression in ERAqPET Positive	P value	Bonferroni Correction (n=119)
miR-148a-3p	6926.34	13,798.83	1.99	4.65E-07	0.000055
miR-223-3p	51723.05	95,960.92	1.86	0.046	5.474
miR-345-5p	276.12	472.19	1.71	0.046	5.474
miR-143-3p	1848.78	3032.05	1.64	0.017	2.023
miR-629-5p	638.11	946.09	1.48	0.024	2.856
miR-24-3p	1817.41	2606.93	1.43	0.015	1.785
miR-140-5p	151.11	205.77	1.36	0.037	4.403
miR-190b	90.94	121.87	1.34	0.012	1.428
miR-181a-5p	395.28	511.04	1.29	0.046	5.474
miR-27b-3p	378.04	480.41	1.27	0.03	3.57
miR-144-3p	142.95	92.33	−1.55	0.015	1.785
let-7e-5p	651.16	429.94	−1.51	0.0094	1.118
miR-98-5p	292.34	193.18	−1.51	0.0019	0.226
miR-4732-3p	219.06	147.46	−1.49	0.033	3.927
miR-142-3p	9443.37	6459.67	−1.46	0.0083	0.987
miR-374a-5p	64.11	44.41	−1.44	0.0031	0.368
miR-125a-5p	2423.26	1715.27	−1.41	0.021	2.499
miR-126-5p	1666.13	1201.74	−1.39	0.0094	1.118
miR-26b-5p	3772.61	2722.64	−1.39	0.00041	0.048
miR-20a-5p	460.29	332.73	−1.38	0.015	1.785
miR-15a-5p	846.79	620.21	−1.37	0.024	2.856
let-7f-5p	21834.73	17,062.88	−1.28	0.027	3.213
miR-103a-3p	5612.37	4611.09	−1.22	0.037	4.403
miR-26a-5p	4157.2	3556.91	−1.17	0.013	1.547

miR-126-5p, miR-374a-5p, miR-26b-5p, miR-98-5p, miR-125a-5p, miR-142-3p, miR-26a-5p, miR-15a-5p, and miR-20a-5p—were downregulated in the ERAqPET-positive cohort. Unsupervised hierarchical clustering and PCA of these miRNAs distinctly separated adequate and inadequate responders (Figure 1A and B). Additional PCA projections using higher-order principal components (PC3 vs. PC4) demonstrated consistent group separation (Figure S3).

To prioritize candidates, we focused on miR-148a-3p, which exhibited the greatest expression difference between ERAqPET groups (Bonferroni-corrected $p = 5.5\times10^{-5}$) (Figure 1C). Linear regression revealed a significant positive correlation between baseline miR-148a-3p expression and qPET metabolic parameters (Spearman $p = 1.43\times10^{-5}$) (Figure 1D). After induction therapy, miR-148a-3p expression did not differ between the ERAqPET groups (Figure

https://doi.org/10.2147/ITT.S577426

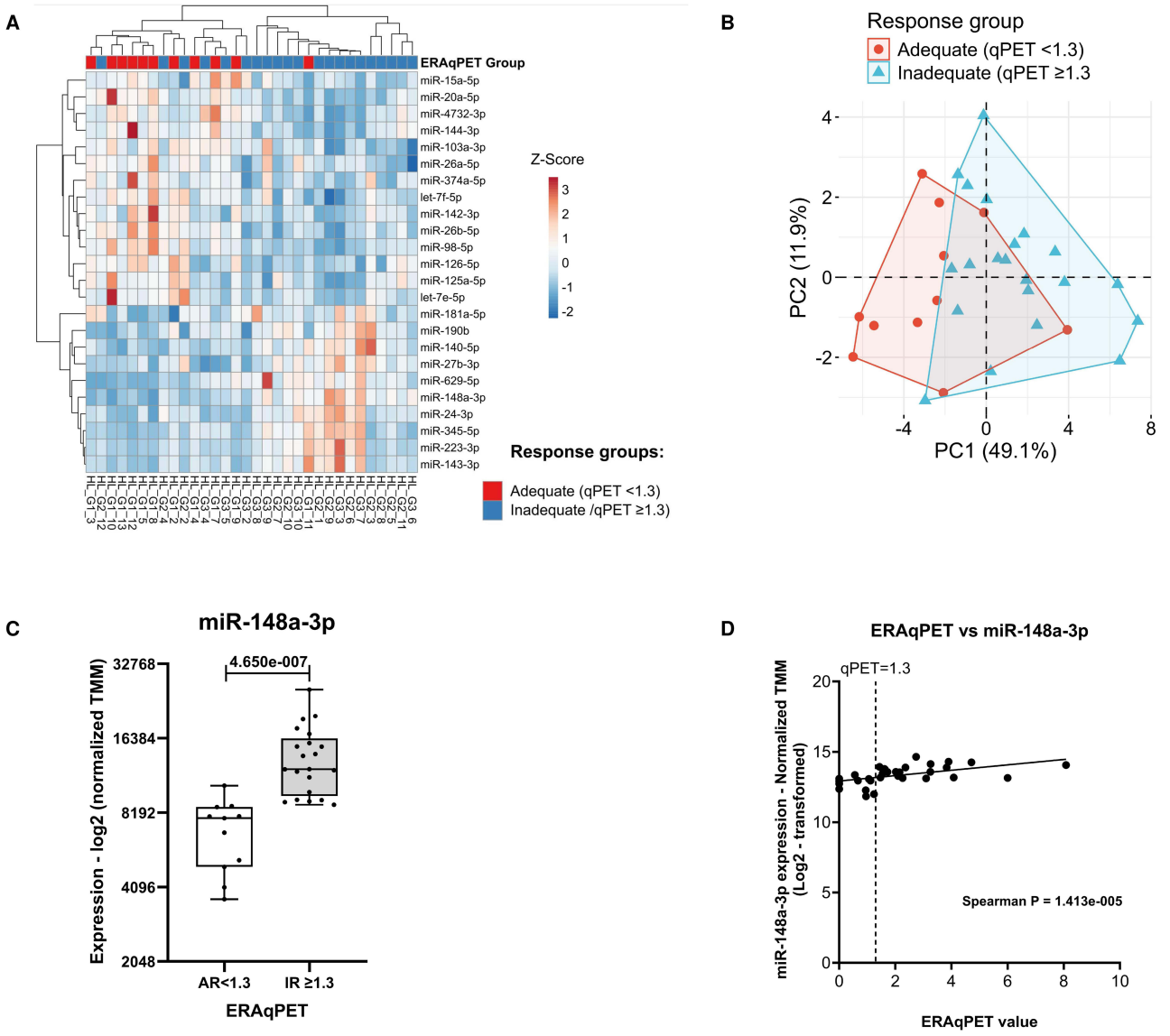

Figure 1 Baseline serum-miRNA profiling distinguishes ERAqPET-positive and -negative Hodgkin lymphoma patients and predicts post-Induction PET response via miR-148a-3p. (**A**) Heat map and hierarchical clustering by samples and miRNAs were performed on the listed samples (bottom) using the 24 differentially expressed miRNAs (Left) based on normalized TMM counts for each miRNA for each patient analyzed from qPET <1.3 (Red) and qPET ≥1.3 (Blue) groups. The colour scale shown (in Log fold) illustrates the relative expression level of the indicated miRNA across all samples: Blue indicates low expression of miRNA, and red indicates high expression of miRNA. (**B**) Principal component analysis plot for 24 significantly differentially expressed miRNAs in adequate responder (AR) and inadequate responder (IR) patients. Patient's samples from ERAqPET negative <1.3 (Red dots) and ERAqPET positive ≥1.3 (Blue triangles) groups cluster separately, with a closer relationship of patients with each other. (**C**) Baseline miR-148a-3p expression at diagnosis (Day 0). Box plots display normalized read counts (TMM values) for miR-148a-3p. Boxes represent interquartile ranges (Tukey method), horizontal lines indicate medians, and whiskers show data ranges. Significant differential expression between groups is indicated ($p < 0.05$). (**D**) Linear regression shows association between pre-treatment miR-148a-3p expression and post-OEPA ERAqPET response in HL patients. Scatter plot show normalized expression (Log2-transformed TMM values) of miR-148a-3p (y-axis) versus ERAqPET scores (x-axis). Spearman's rank correlation test was performed for statistical significance ($p < 0.05$).

S4A). However, the longitudinal analysis showed significant shifts in change of expression between both the groups (Figure S4B), predominantly underscoring its predictive value at baseline.

qRT-PCR validation confirmed elevated baseline miR-148a-3p levels in inadequate responders. However, post-treatment differences were abrogated (Figure 2A), reinforcing its potential as a baseline biomarker. High ERAqPET values at diagnosis were associated with B symptoms ($p = 0.017$), extranodal lesions ($p = 0.0009$), elevated ESR ≥30 mm/h ($p = 0.019$), and bulky disease ($p = 0.026$); Figure 2B). qRT-PCR data for miR-148a-3p confirmed associations

https://doi.org/10.2147/ITT.S577426

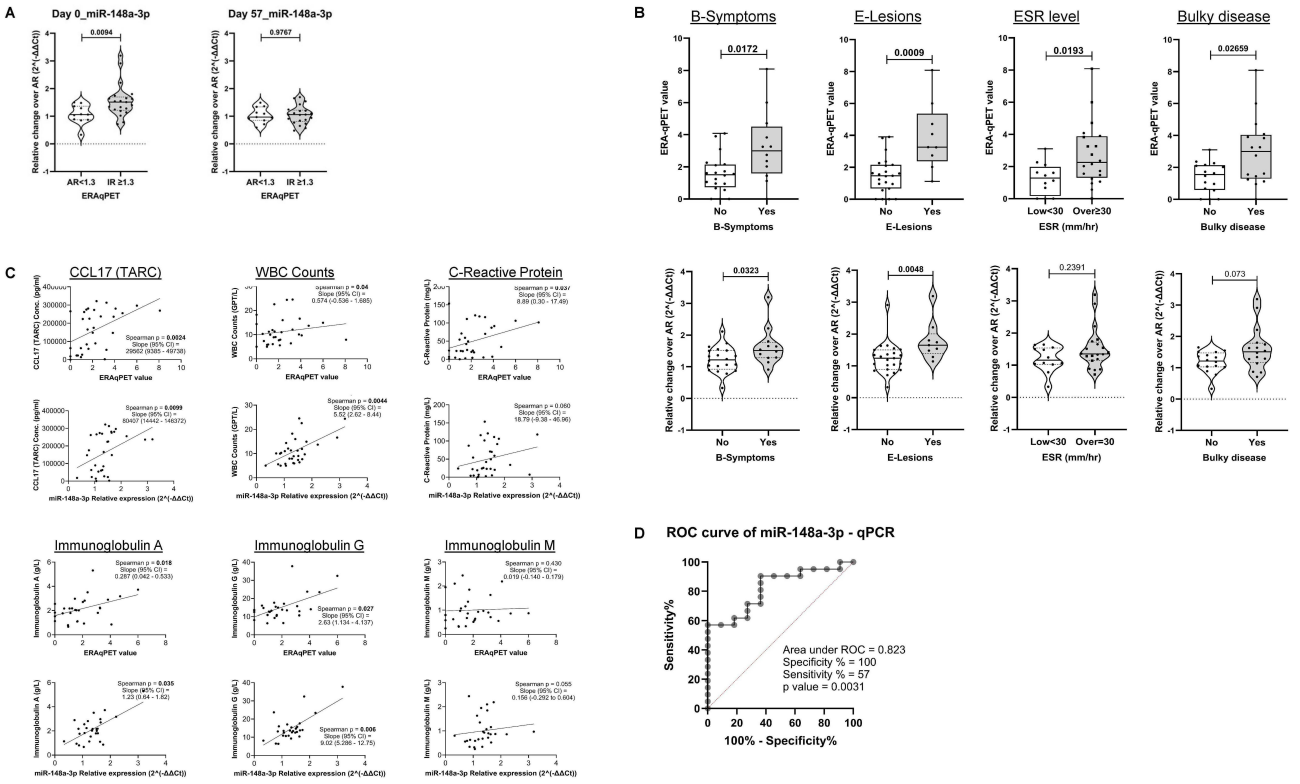

Figure 2 qRT-PCR–validated serum miR-148a-3p and early PET response differentiate responders from non-responders to OEPA induction-therapy in Hodgkin lymphoma. (**A**) miR-148a-3p expression dynamics during induction therapy. Relative miR-148a-3p expression levels at diagnosis (Day 0) and after induction therapy (Day 57), normalized to the mean of the ERAqPET-negative (AR) group. Violin plots show the distribution of values; violins indicate interquartile ranges (Tukey method), solid horizontal lines mark medians, and whiskers denote data ranges (dashed for violins). Statistically significant differences between groups ($p < 0.05$) are annotated. (**B**) Comparison analysis: Early response qPET and baseline miR-148a-3p expression across clinical subgroups. Upper panels: early response qPET values. Lower panels: baseline miR-148a-3p expression in the same subgroups, normalized to the mean of the ERAqPET-negative (AR) group. Violin plots display relative expression changes. Boxes and violins represent interquartile ranges (Tukey method), solid horizontal lines indicate medians, and whiskers show data ranges (dashed for violins). Significant differences between groups ($p < 0.05$) are indicated. (**C**) Correlation analysis: Upper panels show association between treatment response (qPET) on the x-axis and clinical parameters on the y-axis and lower panels show association between baseline miR-148a-3p expression and corresponding clinical parameters. Correlation plots show relative miRNA expression (2^(-ΔΔCt) values) on the x-axis versus corresponding clinical values on the y-axis. Statistical significance was assessed using Spearman's rank correlation test ($p < 0.05$). (**D**) Receiver operating characteristic (ROC) curve for miR-148a-3p levels. ROC analysis was performed using qRT-PCR data to evaluate the diagnostic performance of miR-148a-3p. The black solid line represents the experimental ROC curve; the red dashed line represents the identity line (AUC = 0.5). Area under the ROC curve (AUC), p-value, and sensitivity/specificity percentages at the selected threshold are indicated.

with B symptoms ($p = 0.03$) and extranodal lesions ($p = 0.004$), although ESR ($p = 0.239$) and bulky disease ($p = 0.073$) did not reach significance (Figure 2B).

Linear regression analysis revealed significant positive associations between baseline miR-148a-3p expression and several clinical markers; these relationships were corroborated by Spearman's rank correlation. Baseline miR-148a-3p correlated with serum CCL17 (thymus- and activation-regulated chemokine, TARC) ($p = 0.009$), white blood cell (WBC) count ($p = 0.0044$), immunoglobulin A ($p = 0.035$), and immunoglobulin G ($p = 0.006$). No significant correlations were observed with C-reactive protein (CRP) ($p = 0.06$) or immunoglobulin M ($p = 0.055$) (Figure 2C), highlighting its association with some selective inflammatory and immunological disease features. Box plot analysis confirmed that miR-148a-3p levels remained stable across age and sex. This indicates that the miR-148a-3p associated with ERAqPET status is independent of these demographic variables (Figure S5).

ROC analysis was performed to assess whether miR-148a-3p expression is associated with metabolic response following OEPA induction therapy. The curve demonstrated separation between groups (Figure 2D), with an AUROC of 0.823 (95% CI 0.677–0.967), a sensitivity of 0.57, and a specificity of 1.00 for distinguishing adequate responders from inadequate responders. The association was statistically significant ($p = 0.0031$), indicating that miR-148a-3p may serve to distinguish responders within this cohort.

https://doi.org/10.2147/ITT.S577426

Discussion

The current management of pediatric high-risk cHL requires precise approaches that integrate polychemotherapy and radiotherapy de-escalation[1,2] with novel immunotherapy agents to optimize efficacy and minimize long-term toxicity.[12] Although quantitative 18F-FDG-PET serves as the gold standard for response assessment,[7] serum-based miRNA profiling has emerged as a promising adjunct for monitoring treatment responses in various malignancies.[13]

Our pilot study demonstrated that pre-treatment circulating miRNA signatures can discriminate between adequate and inadequate responders after two OEPA-cycles, effectively "rediscovering" several circulating and tissue-specific miRNAs previously implicated in adult cHL.[5,6] These results suggest that pretreatment miRNA profiles could complement early risk stratification.

Among the differentially expressed miRNAs, miR-148a-3p is of particular interest as it functions as either a tumor suppressor or an oncogene in a context-dependent manner.[14] In various cancers, including cHL, miR-148a-3p is frequently downregulated by DNA methylation–mediated epigenetic silencing compared to non-malignant cells, which affects pathways involved in cell proliferation, migration, and invasion.[14,15]

Paradoxically, our pediatric cohort exhibited elevated baseline serum miR-148a-3p levels, specifically among the inadequate responders. This may reflect the heterogeneous methylation patterns previously reported in cHL: Paczkowska et al documented methylation-induced silencing of miR-148a-3p in four of seven cHL cell lines and two of six primary Hodgkin and Reed/Sternberg (HRS) cell samples compared with non-malignant cells.[15] Alternatively, high serum levels may originate from non-malignant sources, highlighting its potential role as a biomarker for aggressive, pro-tumorigenic disease. Although often downregulated in most cancers, miR-148a-3p is upregulated in glioma, osteosarcoma, and prostate cancer, where higher expression correlates with advanced stage and poorer prognosis.[16–18]

Mechanistically, miR-148a-3p directly targets critical tumor suppressors, such as DNA methyltransferase 1 (DNMT1) and phosphatase and tensin homolog (PTEN), binding to their 3′-untranslated regions (UTRs) to inhibit translation.[19] By suppressing DNMT1, miR-148a-3p induces global DNA hypomethylation, a recognized epigenetic hallmark of tumorigenesis.[20,21] Beyond epigenetic regulation, miR-148a-3p overexpression may facilitate HRS cell immune escape by downregulating β-microglobulin and impairing HLA class I expression, as demonstrated in colorectal tumors.[22] Additionally, it regulates B cell differentiation via targets such as BACH2, MITF, BIM, and PTEN,[23] potentially linking it to the aberrant B cell transcriptional program characteristic of cHL.

Elevated baseline miR-148a-3p levels in our cohort were associated with higher CCL17/TARC levels, an established pediatric-cHL diagnostic marker,[24] as well as increased Immunoglobulin G and Immunoglobulin A titers, both of which are recognized features of Hodgkin lymphoma.[25,26] The association with B-symptoms and extranodal involvement further supports its link to aggressive disease features. Importantly, age and sex did not appear to influence baseline miR-148a-3p expression, suggesting that the observed associations with metabolic response are unlikely to be driven by demographic confounding.

Furthermore, diagnostic performance analyses indicate an association between miR-148a-3p expression and metabolic response. While these results suggest that miR-148a-3p may help to distinguish responders from non-responders within this cohort, validation in larger, independent patient populations will be required before clinical applicability can be inferred. Future studies may explore whether integrating miR-148a-3p into broader panels of soluble biomarkers could enhance multi-parametric strategies for early risk assessment in pediatric cHL.

Conclusion

Our preliminary findings indicate that circulating miR-148a-3p levels at diagnosis are associated with metabolic tumor activity, inflammatory markers, and adverse clinical features in pediatric cHL. These observations suggest that miR-148a-3p may contribute to multi-parametric biomarker approaches aimed at the early identification of patients at risk for delayed metabolic remission. The decline of elevated pre-treatment levels following induction therapy is consistent with an association with disease burden, although its predictive relevance requires confirmation. Given the exploratory nature of this pilot study, validation in larger, independent cohorts will be necessary to define its biological and potential clinical utility.

Study Period of Research

The study patients were enrolled in the EuroNet-PHL-C2 trial and samples were collected between February 2016 and February 2019 at multiple clinical centers in Germany.

Data Sharing Statement

The original contributions of this study are included in the article and Supplementary Material. Further inquiries can be directed to the corresponding author. The small RNA sequencing data were submitted to the GEO repository under accession number GSE308257.

Ethical Approval and Patient Consent

This study was conducted in accordance with the principles of the Declaration of Helsinki. Ethics approval for the EuroNet-PHL-C2 trial and associated studies was granted by the Ethics Committee of Martin-Luther-University Halle-Wittenberg, Germany (reference 2015-12) and by the Ethics Committee of Justus-Liebig-University Giessen, Germany, reference 289/20.

All procedures adhered to institutional ethical standards, and age-appropriate information was provided before informed consent was obtained from the participants and their legal guardians.

Acknowledgments

We thank the patients, their parents, and the participating clinics in the EuroNet-PHL-C2 study. We are grateful to Simone Schwalm, Department of Pediatric Hematology and Oncology, Justus-Liebig University, Giessen, Germany for her excellent technical support. During the preparation of manuscript, the authors used Microsoft Copilot (https://copilot.microsoft.com/) to improve the readability and language of this manuscript. The authors reviewed and edited the manuscript and took full responsibility for its final publication.

Author Contributions

All authors have made significant contributions to the reported work, including its conception, study design, execution, data acquisition, and analysis and interpretation. Each author participated in drafting, revising, or critically reviewing the manuscript; gave final approval of the version to be published; agreed on the journal for submission; and accepts accountability for all aspects of the work.

Funding

The authors gratefully acknowledge financial support from Elternverein für leukämie- und krebskranke Kinder, Gießen e. V., which funded M.R., V.K.S., and D.K. Additional support for V.K.S. and A.W. was provided by Forschungshilfe Peiper, Department of Pediatric Oncology, Hematology, and Immunodeficiencies, Justus-Liebig University, Giessen, Germany.

Disclosure

Prof. Dr. Christine Mauz-Körholz reports grants from MSD Pharma, outside the submitted work; and Leadership (unpaid): Scientific Secretary of the EuroNet-PHL group (European network for Pediatric Hodgkin lymphoma). The authors declare no other conflicts of interest in this work.

References

1. Mauz-Korholz C, Landman-Parker J, Fernandez-Teijeiro A, et al. Response-adapted omission of radiotherapy in children and adolescents with early-stage classical Hodgkin lymphoma and an adequate response to vincristine, etoposide, prednisone, and doxorubicin (EuroNet-PHL-C1): a titration study. *Lancet Oncol*. 2023;24(3):252–261. doi:10.1016/S1470-2045(23)00019-0
2. Mauz-Korholz C, Landman-Parker J, Balwierz W, et al. Response-adapted omission of radiotherapy and comparison of consolidation chemotherapy in children and adolescents with intermediate-stage and advanced-stage classical Hodgkin lymphoma (EuroNet-PHL-C1): a titration study with an open-label, embedded, multinational, non-inferiority, randomised controlled trial. *Lancet Oncol*. 2022;23(1):125–137. doi:10.1016/S1470-2045(21)00470-8

3. Peng Y, Croce CM. The role of MicroRNAs in human cancer. *Signal Transduct Target Ther*. 2016;1(1):15004. doi:10.1038/sigtrans.2015.4
4. Anfossi S, Babayan A, Pantel K, Calin GA. Clinical utility of circulating non-coding RNAs - an update. *Nat Rev Clin Oncol*. 2018;15(9):541–563. doi:10.1038/s41571-018-0035-x
5. Cordeiro A, Monzo M, Navarro A. Non-Coding RNAs in Hodgkin Lymphoma. *Int J Mol Sci*. 2017;18(6):1154. doi:10.3390/ijms18061154
6. Pan Y, Cengiz R, Kluiver J, Diepstra A, Van den Berg A. Pinpointing Functionally Relevant miRNAs in Classical Hodgkin Lymphoma Pathogenesis. *Cancers*. 2024;16(6):1126. doi:10.3390/cancers16061126
7. Kurch L, Landman-Parker J, Georgi TW, et al. Quantitative Deauville Scoring to Uncover Prognostic Information from (18)F-FDG PET-Based Response Assessment: data from the EuroNet-PHL-C1 Trial. *J Nucl Med*. 2025;66(9):1331–1337. doi:10.2967/jnumed.125.269603
8. Blondal T, Jensby Nielsen S, Baker A, et al. Assessing sample and miRNA profile quality in serum and plasma or other biofluids. *Methods*. 2013;59 (1):S1–6. doi:10.1016/j.ymeth.2012.09.015
9. Pantano L, Estivill X, Marti E. A non-biased framework for the annotation and classification of the non-miRNA small RNA transcriptome. *Bioinformatics*. 2011;27(22):3202–3203. doi:10.1093/bioinformatics/btr527
10. Keller A, Rounge T, Backes C, et al. Sources to variability in circulating human miRNA signatures. *RNA Biol*. 2017;14(12):1791–1798. doi:10.1080/15476286.2017.1367888
11. Robinson MD, McCarthy DJ, Smyth GK. edgeR: a Bioconductor package for differential expression analysis of digital gene expression data. *Bioinformatics*. 2010;26(1):139–140. doi:10.1093/bioinformatics/btp616
12. Kahn JM, Mauz-Korholz C, Hernandez T, Milgrom SA, Castellino SM. Pediatric and Adolescent Hodgkin Lymphoma: paving the Way for Standards of Care and Shared Decision Making. *Am Soc Clin Oncol Educ Book*. 2024;44(3):e432420. doi:10.1200/EDBK_432420
13. Chakrabortty A, Patton DJ, Smith BF, Agarwal P. miRNAs: potential as Biomarkers and Therapeutic Targets for Cancer. *Genes*. 2023;14(7):1375. doi:10.3390/genes14071375
14. Li Y, Deng X, Zeng X, Peng X. The Role of Mir-148a in Cancer. *J Cancer*. 2016;7(10):1233–1241. doi:10.7150/jca.14616
15. Paczkowska J, Janiszewska J, Bein J, et al. The Tumor Suppressive mir-148a Is Epigenetically Inactivated in Classical Hodgkin Lymphoma. *Cells*. 2020;9(10):2292. doi:10.3390/cells9102292
16. Hua D, Mo F, Ding D, et al. A catalogue of glioblastoma and brain MicroRNAs identified by deep sequencing. *OMICS*. 2012;16(12):690–699. doi:10.1089/omi.2012.0069
17. Ma W, Zhang X, Chai J, Chen P, Ren P, Gong M. Circulating miR-148a is a significant diagnostic and prognostic biomarker for patients with osteosarcoma. *Tumour Biol*. 2014;35(12):12467–12472. doi:10.1007/s13277-014-2565-x
18. Dybos SA, Flatberg A, Halgunset J, et al. Increased levels of serum miR-148a-3p are associated with prostate cancer. *APMIS*. 2018;126 (9):722–731. doi:10.1111/apm.12880
19. Gurbuz V, Sozen S, Bilen CY, Konac E. miR-148a, miR-152 and miR-200b promote prostate cancer metastasis by targeting DNMT1 and PTEN expression. *Oncol Lett*. 2021;22(5):805. doi:10.3892/ol.2021.13066
20. Saviana M, Le P, Micalo L, et al. Crosstalk between miRNAs and DNA Methylation in Cancer. *Genes*. 2023;14(5):1075. doi:10.3390/genes14051075
21. Lee E, Wang J, Yumoto K, et al. DNMT1 Regulates Epithelial-Mesenchymal Transition and Cancer Stem Cells, Which Promotes Prostate Cancer Metastasis. *Neoplasia*. 2016;18(9):553–566. doi:10.1016/j.neo.2016.07.007
22. Zheng J, Yang T, Gao S, et al. miR-148a-3p silences the CANX/MHC-I pathway and impairs CD8(+) T cell-mediated immune attack in colorectal cancer. *FASEB J*. 2021;35(8):e21776. doi:10.1096/fj.202100235R
23. Murata T, Takayama K, Katayama S, et al. miR-148a is an androgen-responsive microRNA that promotes LNCaP prostate cell growth by repressing its target CAND1 expression. *Prostate Cancer Prostatic Dis*. 2010;13(4):356–361. doi:10.1038/pcan.2010.32
24. Plattel WJ, Visser L, Diepstra A, et al. Interim thymus and activation regulated chemokine versus interim (18) F-fluorodeoxyglucose positron-emission tomography in classical Hodgkin lymphoma response evaluation. *Br J Haematol*. 2020;190(1):40–44. doi:10.1111/bjh.16514
25. Zijtregtop EAM, Meyer-Wentrup F, Wong WC, et al. Plasma thymus and activation-regulated chemokine (TARC) as diagnostic marker in pediatric Hodgkin lymphoma. *EJHaem*. 2020;1(1):152–160. doi:10.1002/jha2.41
26. Wagener DJ, Van Munster PJ, Haanen C. The immunoglobulins in Hodgkin's disease. *Eur J Cancer*. 1976;12(9):683–688. doi:10.1016/0014-2964(76)90016-5